Journal of Applied Polymer Science

Foam Stability and Polymer Phase Morphology of Flexible Polyurethane Foams Synthesized from Castor Oil

Chandan Sharma,[1] Sanjay Kumar,[1] A. Raman Unni,[2] Vinod K. Aswal,[3] Sangram K. Rath,[4] G. Harikrishnan[1]

[1]Department of Chemical Engineering, Indian Institute of Technology Kharagpur, Kharagpur, West Bengal 721302, India
[2]Automotive and Flexible Foam Division, Huntsman Polyurethanes, Navi Mumbai, Maharashtra 400710, India
[3]Solid State Physics Division, Bhabha Atomic Research Centre, Mumbai, Maharashtra 400085, India
[4]Polymer Division, Naval Materials Research Laboratory, Ambernath, Maharashtra 421506, India
Correspondence to: G. Harikrishnan (E-mail: hari@iitkgp.ac.in)

ABSTRACT: Foam stability and segmented polymeric phase morphology of polyurethane foams synthesized partially and completely from castor oil are investigated. Preliminary analysis of the impact of alterations in the polymeric phase on macroscopic stress dissipation in foams is also carried out. The stability and morphology show unique trends depending on the concentration of castor oil used in foam synthesis. While low and intermediate concentrations of castor oil does not significantly affect the foaming process; at high concentrations, the volumetrically expanding liquid matrix remains in a nonequilibrium state during the entire foaming period, resulting in significant foam decay from top. This increases the final foam cell density and decreases the plateau border thickness at bottom. In the polymeric phase of castor oil based foams, the fraction of monodentate urea increases at the cost of non-hydrogen bonded urea. These monodentate urea domains undergo flocculation in foams synthesized completely from castor oil, thus prominently modifying the segmented morphology. The glass transition temperature of soft segments of partially substituted foams shows moderate increase, with indications of phase mixing between the polyether and castor oil generated urethane domains. Foams synthesized entirely from castor oil have significant sol fraction due to unreacted oligomers. The microscopic alterations in polymeric phase reduce the elastic recovery of partially substituted castor oil foams compared to its viscous dissipation under an applied stress. © 2014 Wiley Periodicals, Inc. J. Appl. Polym. Sci. **2014**, *131*, 40668.

KEYWORDS: biopolymers and renewable polymers; foams; polyurethanes

Received 26 September 2013; accepted 28 February 2014
DOI: 10.1002/app.40668

INTRODUCTION

Foams are the largest used polyurethane product with wide applications traditionally in automobile, furniture, packaging, construction, thermal insulation, footwear, and biomedical realms.[1] Newer applications such as removal of oil from water, in which nanoscopically modified foams could be used are recently reported.[2] In flexible polyurethane foams, the microscopic foam morphological units are pneumatically connected to each other by a segmented polymeric phase, constituting an "open cell" structure. They are synthesized by a reactive foaming process, in which two reactions *viz.* polymerization and foaming, occur simultaneously. Renewable resources such as vegetable oil are fast replacing the conventional fossil fuel derived oligomers in polyurethane synthesis.[3–18] Castor oil is a major candidate in these replacement efforts, due to its inherent advantages over other vegetable oils. The major content of the triglyceride fatty acid residue of castor oil is ricinoleic acid. Ricinoleic acid has inherent hydroxyl groups in their parent hydrocarbon chain due to which the need to introduce hydroxyl groups can be avoided or at least minimize.[4] Moreover, the nonedible nature of castor oil does not affect food security.

A brief survey of the literature on polyurethane foam synthesis from castor oil follows. Some early reports indicate the use of castor oil in making thermally insulating rigid polyurethane foams.[19–21] Castor oil modified with maleic anhydride was used to synthesize biodegradable foams.[22] Diethanol amides of castor oil are reported to be used for water blown polyurethane foams.[23] Castor oil modified by double metal cyanide catalysis shows promises of commercial use.[24] Viscoelastic foams derived by partial replacement shows the same glass transition temperature, higher tensile and tear strengths compared to conventional foams.[25] Castor-oil substituted partially in the synthesis of flexible polyurethane foam resulted in an increase in density and hardness index, but a decrease in tensile strength and elongation.[26] The increased efforts to synthesize polyurethane foams of good quality and performance from castor oil are indicated by the rapid

increase in the literature in the recent times. However, a detailed and fundamental understanding on foaming dynamics and stability as well as the microstructure of the segmented polymeric phase are not available. Such knowledge is essential to make stable foams with tailored properties for various uses and also achieve the goal of complete replacement of fossil fuel derived oligomers. This article investigates these evolutions in flexible polyurethane foams synthesized partially and completely from castor oil. The impact of changes in polymer morphology on foam stress dissipation under an applied load is additionally analyzed. For this, a series of foams from a conventional polyol, its blend with castor oil and finally pure castor oil, were synthesized. This was facilitated by a gradual replacement of a commercially used polyether polyol by castor oil.

MATERIALS AND METHODS

Materials

Hydroxyl oligomer with a polyether backbone (polypropylene glycol based, Konix FA 505, KPX Chemicals, S. Korea) having approximate functionality, hydroxyl value and molecular weight of 3.0, 35 mg KOH/g polyol, and 4700, respectively and isocyanate (oligomeric 4,4′ diphenyl methane diisocyanate, Suprasec 6456, Huntsman, NCO content: 30.4%) were used. Castor oil used (Loba Chemie) had an approximate functionality of 2.7, hydroxyl value of 163 mg KOH/g oil and molecular weight of 930. Foaming agents used contained a surfactant (Tegostab 8734 LF, Evonik), catalysts that include bis(2-dimethylaminoethyl)ether (Niax A1, Momentive), diethanolamine (Sigma-Aldrich) and a mixture of triethylenediamine and dipropyleneglycol (Dabco 33LV, Air Products). Distilled water was used as the foaming agent.

Foaming

The polyol component was prepared by adding the hydroxyl oligomer (93.3 parts by weight (pbw)), distilled water (4.2 pbw), catalyst blend (NIAX A1 = 0.1 pbw, diethanolamine = 0.3 pbw, Dabco 33 LV = 0.35 pbw) and surfactant (0.5 pbw) into a paper cup of volume 600 mL. The blend was homogenized with a high speed stirrer (RQ-122, Remi) at an approximate speed of 3000 rpm. Following that, the isocyanate oligomer was added to the blend in the ratio 65:100 and stirred at a high speed of 4000 rpm for 15 s. The foam was allowed to expand freely and was kept for curing at room temperature. For synthesizing castor oil based foams, progressive replacement of polyether polyol with castor oil was conducted. To observe the effect of transient development of liquid matrix modulus on foam stability, delayed foaming experiments were also conducted. To execute this, the foaming reaction was preferentially delayed *vis a vis* polymerization. Polyol blend that is devoid of water was stirred with isocyanate and while the polymerizing reaction was proceeding, distilled water was added after specific short time (during the pregel period) and stirred again. For making foams suitable for load bearing properties, the reacting mixture was poured into a preheated (45°C) mold of size 380 × 380 × 75 cm^3. The mold was closed quickly and the foam was removed after at least 5 min. Foams synthesized completely from polyether polyol and castor oil are designated as P-PUF and C-PUF, respectively and those from blends are designated as *x*CP-PUF, where "*x*" indicates the weight fraction of castor oil in the hydroxyl component.

Characterizations

The steady shear rheology of hydroxyl components and the development of viscoelasticity of nonfoaming system were carried out by a Rheometer (Anton Paar Physica MCR 301). For linear viscoelasticity measurements of a nonfoaming system, after stirring the polyol blend (without water) with isocyanate, the polymerizing liquid was immediately injected between the parallel plates of the Rheometer. The *in situ* development of storage and loss moduli was monitored by small strain oscillatory time sweep experiments at constant frequency. The microscopic foam morphology was imaged by scanning electron microscopy (JEOL JSM 5800). Samples of size 5 × 10 × 2 mm^3 were cut from foam buns at a height of 5 cm from the bottom. Imaging was done in a direction normal to the foam rise. Foams, whose height was <5 cm were designated as collapsed/unstable and were not imaged. The cell number density (CND) and mean strut thickness (MST) was calculated from scanning electron micrographs, using image analysis software (ImageJ) by a method described elsewhere.[27] The sol fraction in the polymeric phase was estimated by solvent extraction. The dried samples were immersed in dimethyl formamide for a period of 3 days. The samples were then kept in a vacuum oven at 80°C for 2 days. The sol fraction was calculated based on the difference in weight. Fourier transform infrared spectrometer (Spectrum 100, Perkin Elmer) was used to collect infrared spectra of foam samples. The deconvolution of the spectra was conducted by a software (MagicPlot). The glass transition in polymeric phase was estimated by measuring the dissipation factor (tan δ) of the foam samples using a dynamic mechanical analyzer (Gabo, Eplexor 100 N) over a temperature range of −80 to 50°C at a frequency of 1 Hz, a ramp rate of 3°C min^{-1} and an initial strain of 0.2%. The segmented polymeric phase of the foam was analyzed by atomic force microscope. Because a porous foam sample cannot be used in force microscopy, films suitable for AFM imaging from a foaming liquid is prepared using a "collapsed foam" technique described elsewhere.[28] Phase imaging of these films were conducted by tapping mode atomic force microscope (Agilent technologies, Model 5100). The polymeric phase was further analyzed by small angle neutron scattering. The wavelength of mean incident radiation was 5.2 Å with $\Delta\lambda/\lambda = 15\%$. The range of scattering vector (Q) was between 0.017 and 0.35 $Å^{-1}$. The scattering data were corrected for the background, the empty cell contributions, transmission and were placed on an absolute scale using standard protocols. Analysis of the scattering data was carried out by considering the corrections due to instrument smearing. The load bearing capacity of molded foams that are cured for 2 days are carried out by a universal testing machine (Instron 3365) using a parallel plate indenter (ISO 2439).

RESULTS AND DISCUSSIONS

Foam Stability

The stability of a reactively foamed polymer is a complex function of several parameters including transient viscosity buildup, the competition between polymerization and foaming (volume

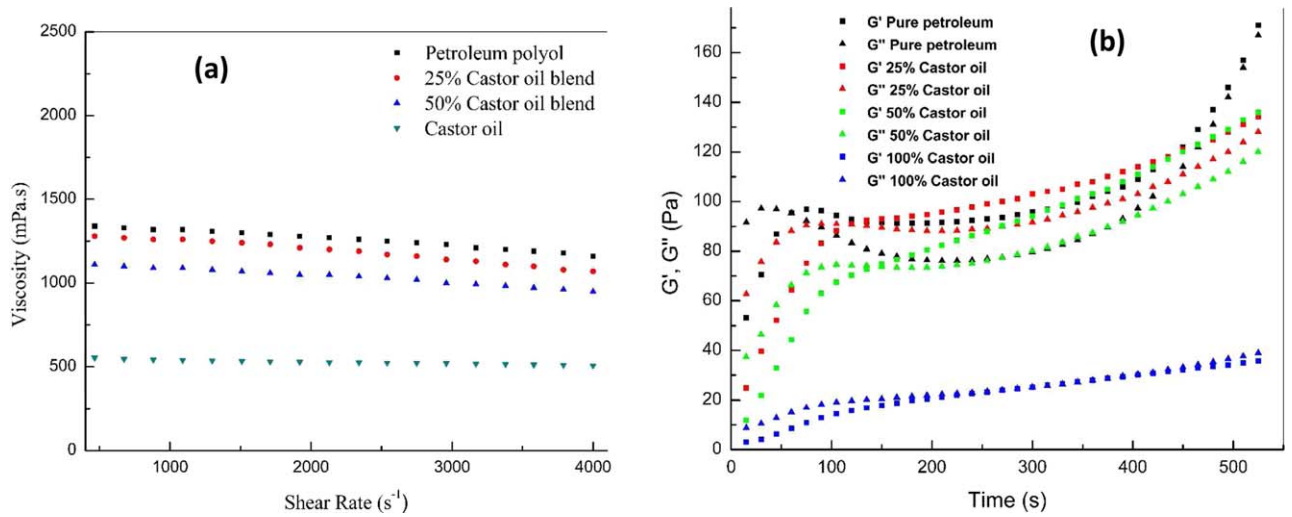

Figure 1. (a) Steady shear rheology of hydroxyl components: (b) viscoelastic developments during polymerization of a nonfoaming system. [Color figure can be viewed in the online issue, which is available at wileyonlinelibrary.com.]

expansion) reactions, bubble growth, bubble coalescence etc. We analyze the foam stability by a combined investigation of viscosity of hydroxyl component, *in situ* development of viscoelasticity of non-foaming system, delayed foaming experiments, final foam height, plateau border (strut) thickness and foam cell density.

Figure 1(a) shows the steady shear rheology of pure polyether polyol, castor oil and their blends. All hydroxyl components are Newtonian in behavior, showing negligible variation of viscosity with shear rate. However, the constant Newtonian viscosity of pure castor oil is significantly less ($\eta_{\text{poyeth.polyol}}/\eta_{\text{castor.oil}} = 2.3$). The viscosity of the blends decreases with increasing concentration of castor oil. Figure 1(b) shows the transient development of viscoelastic moduli of a non-foaming system. The gelation of the polymerizing network as indicated by the adiabatic gel time at which there is no equilibrium modulus is sharply defined (at ~60 s) in the case of pure polyether polyol. The time required for completion of gelation increases with increasing concentration of castor oil. The rate of development of storage and loss modulus shows substantial reduction when pure castor oil is used. The gelation is only partially complete, even at very high time duration. This indicates insufficient molecular weight buildup and crosslinking during the period of foaming. While the transient viscoelastic development of a nonfoaming network is used here for analyzing foam stability, caution is necessary. Under nonfoaming condition (in which the water-isocyanate reaction is absent) the phase behavior of the liquid matrix under rheological investigation may be different from that of a foaming liquid. This is due to the absence of carbamic acid that is a product of the reaction of water with isocyanate functional groups. Hence, the viscoelastic developments of a non-foaming network should only be considered as qualitatively indicative, but not exactly replicating the rheological behavior of a foaming system. However, this technique is useful as the shear rheological investigation of a foaming mixture can lead to erroneous results due to the nucleation of gas bubbles.

The height of the free rise foams gives a visual indication of the relative foam stability. For concentrations within 25% of castor oil, the foam height shows negligible change compared to conventional foams. However beyond this, the height starts decreasing. A substantial reduction in foam height indicates foam decay due to increasing bubble coalescence and rupture at the top of the foam bun. Figure 2 shows the scanning electron micrographs of foam specimens removed from a constant height (5 cm) from the bottom. The estimated cell number densities and mean strut thickness are shown in bracket. The cell density of *50*CP-PUF is 84% higher compared to that of P-PUF. The rapid foam decay and closer packing of cells at high concentrations of castor oil can very well be correlated with the rheological behavior. As described above, a high concentration of castor oil in the hydroxyl component results in low initial viscosity of the reacting components and a rapid decrease in the rate of development of foaming matrix modulus. The water-isocyanate foaming reaction is first order.[29,30] Because the rate of this reaction depends only on the concentration of water which is the limiting reagent, the foaming reaction becomes faster in comparison to that of polymerization. Faster volumetric expansion of the liquid matrix having insufficient modulus causes high rate of foam drainage and lamellar thinning, resulting in bubble coalescence and rupture. The low rate of development of storage modulus mainly affects the elastic strength of the Plateau borders that are formed by the intersection of three bubbles. These Plateau borders, after gelation, become the structural support to foam. The increased liquid drainage as a result of low viscosity buildup at high castor oil content is also clearly manifested by the 36% reduction in the mean Plateau border (strut) thickness in *50*CP-PUF compared to P-PUF. At the top of the foam, the bubble volume is higher and the liquid volume fraction is lesser as compared to the bottom. This is due to increased gas diffusion and liquid drainage respectively.[31] These effects combined together, lead to foam decay from the top, resulting in decrease in final height. This, in turn results in cell units getting closely packed in a reduced volume, increasing the

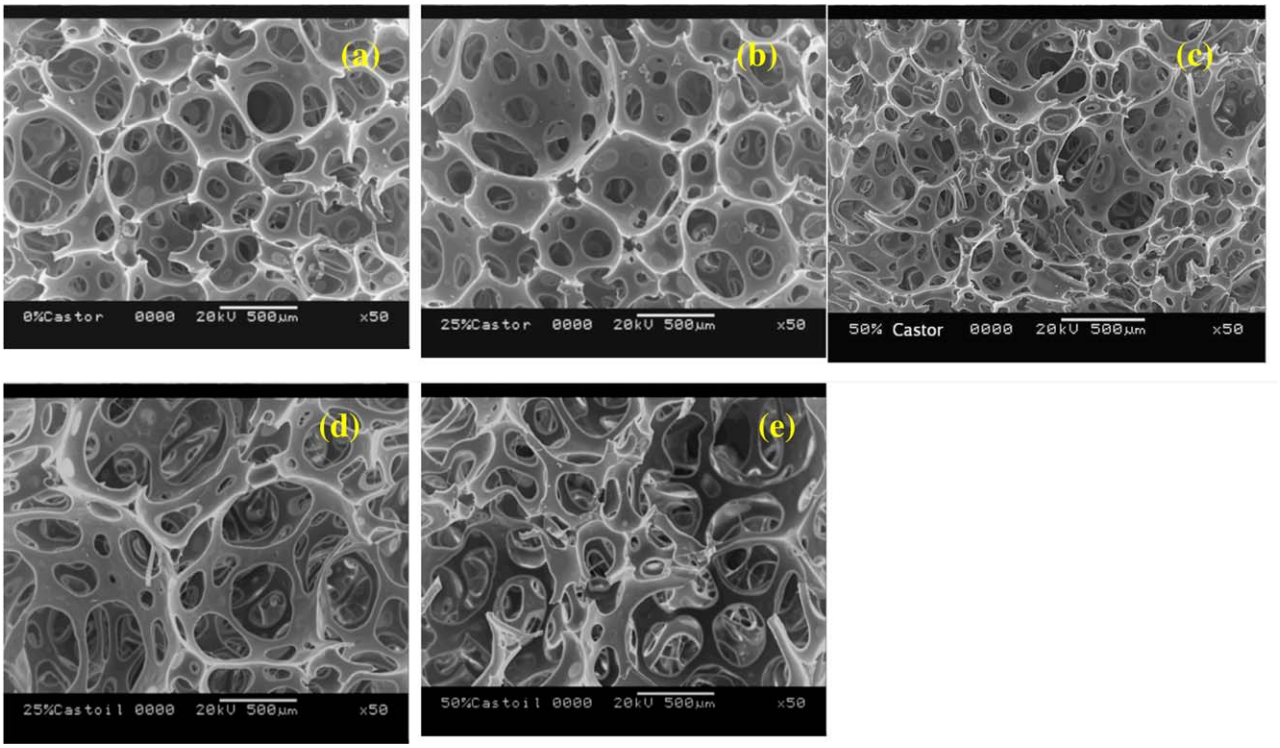

Figure 2. Scanning electron micrographs of foams: (a) P-PUF (CND = 3.1 × 10^{10} cm^{-3}, MST = 53.2 μm); (b) 25CP-PUF (CND = 4.2 × 10^{10} cm^{-3}, MST = 56.5 μm); (c) 50CP-PUF (CND = 5.7 × 10^{10} cm^{-3}. MST = 33.1 μm); (d) *25*CP-PUF (delayed foaming, CND = 3.4 × 10^{10} cm^{-3}, MST = 52 μm); (e) 50CP-PUF (delayed foaming, CND = 4.4 × 10^{10} cm^{-3}, MST = 50.1 μm). CND is cell number density and MST stands for mean strut thickness. [Color figure can be viewed in the online issue, which is available at wileyonlinelibrary.com.]

cell number density. We investigate this further by delayed foaming experiments. Here, the foaming reaction is started at a later time equal to 1/3rd of the gel time that is determined from Figure 2(b). It was possible to increase the final height of the foam bun and hence decrease the foam decay. Figure 2(d,e) shows the cellular morphology of foams obtained by delayed foaming. In stark contrast to the morphology of *50*CP-PUF made by normal foaming process, the cell number density of same foams made by delayed foaming [Figure 2(e)] is closely similar to that of P-PUF [Figure 2(a)]. The mean strut thickness in these foams is also closely similar to that of P-PUF. Hence, when foaming is started at a time, when sufficient moduli are developed, the foam stability is considerably enhanced. Although with delayed foaming, it was possible to enhance the stability and final foam height at relatively high concentrations of castor oil, foams made from 100% castor oil were still unstable and collapsed.

Polymeric Phase

Segmented Morphology. The thermodynamic segmentation of hard and soft blocks during urethane formation has significant influence on foam properties.[32–35] Figure 3 shows the partial FTIR spectra of the foam samples in the wave number region 1600–1800 cm^{-1} (carbonyl stretching). The pertinent band assignments related to various species in a polyurethane network are described in the literature.[36–38] Multiple absorption bands are observed, reflecting the hydrogen bonding between different species. The concentration of bidentate or ordered urea groups is observed to be nominal in all the cases. This is a significant observation as presence of sizeable fraction of ordered or bidentate urea has been reported for similar polyol based foams synthesized from asymmetric toluenediisocyanate.[28] The lack of structural order in the present case with symmetric MDI is most likely of kinetic origin. For the urea domain to self assemble in an ordered fashion by hydrogen bonding, the

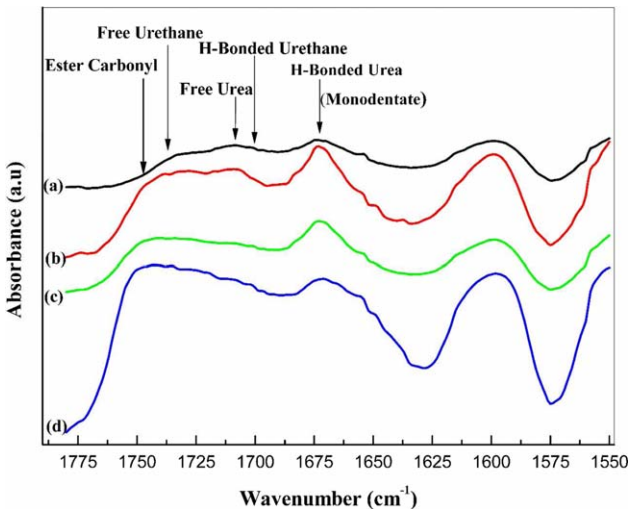

Figure 3. FTIR spectra of foams in the carbonyl stretching region: ((a) P-PUF; (b) 25CP-PUF; (c) 50CP-PUF; (d) C-PUF). [Color figure can be viewed in the online issue, which is available at wileyonlinelibrary.com.]

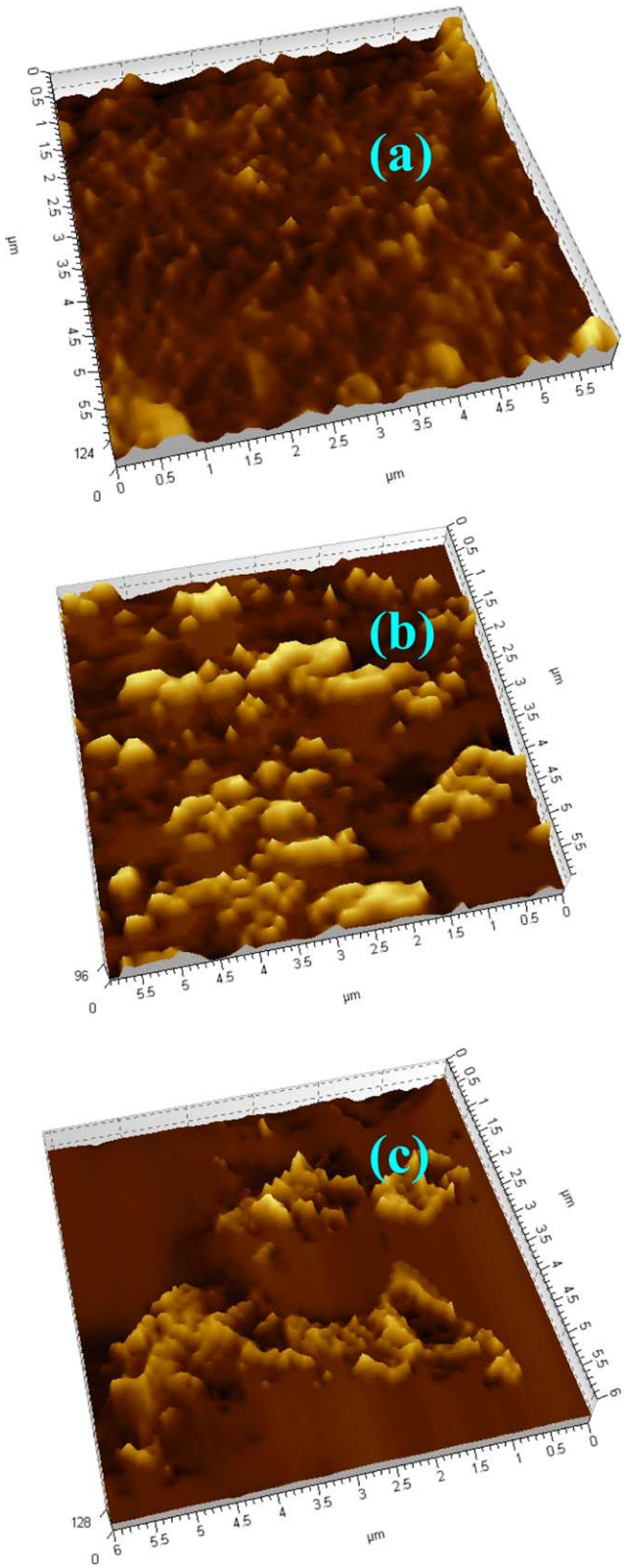

Figure 4. Atomic force micrographs of films made from a foaming mixture: (a) P-PUF, (b) 50CP-PUF and (c) C-PUF. [Color figure can be viewed in the online issue, which is available at wileyonlinelibrary.com.]

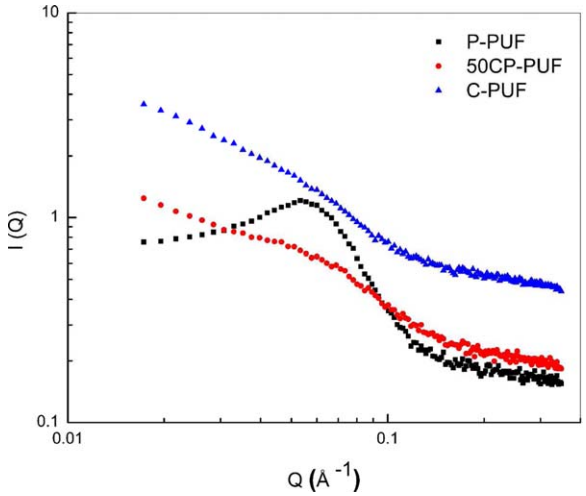

Figure 5. Neutron scattering traces from foams. [Color figure can be viewed in the online issue, which is available at wileyonlinelibrary.com.]

phase separation should take place before the gelation of the network.[39] It is a well known fact that the reactivity of MDI with hydroxyl groups is much higher than that of TDI. A faster reaction can hence prevent the formation of bidentate urea. It is very interesting to note that while the band intensities pertaining to monodentate urea increases with castor oil concentration, those related to free urea (nonhydrogen bonded) decreases, finally disappearing in the case of C-PUF. This clearly indicates an increase in the concentration of hydrogen bonded monodentate urea domain with castor oil substitution.

We now do extended analysis of the segmented morphology by SANS and AFM. Figure 4 shows the atomic force micrographs of films made from a foaming mixture and Figure 5, the neutron scattering traces from foams. The separate domains can be visualized from AFM images based on an established interpretation of modulus-sensitive phase images obtained by light tapping, where the lighter color portions are assigned to the high modulus hard domains and the darker phase to the soft matrix.[28,40] Foams made from pure polyether polyol (P-PUF) shows smaller discrete domains [Figure 4(a)]. In stark contrast, the hard domains in C-PUF show a continuous lamella like structure [Figure 4(c)]. In the case of foams made from blends, an intermediate structure is observed. The discrete domains that were seen in the case of P-PUF are observed to be tending to assemble [Figure 4(b)]. This results in the existence of partially discrete domains with nearly spherical shapes with the rest tending to develop a continuous structure. The SANS traces of foams synthesized from pure polyether polyol show a distinct correlation peak, corresponding to a scattering vector of ~0.08 Å^{-1}. The intensity of the peak is substantially lower (appearing as a shoulder) in the case of *50*CP-PUF. C-PUF does not show such correlation or scattering maxima and is evident from the absence of any discernible peak. The observation of a distinct peak in the case of P-PUF indicates the existence of scattering moieties having well defined geometric identities and are separated in space. The distance of separation between the scattering blocks can be determined as $d = 2\pi/Q_{max}$, where Q_{max} is the value of Q at which $I(Q)$ is maximum. This value (interdomain

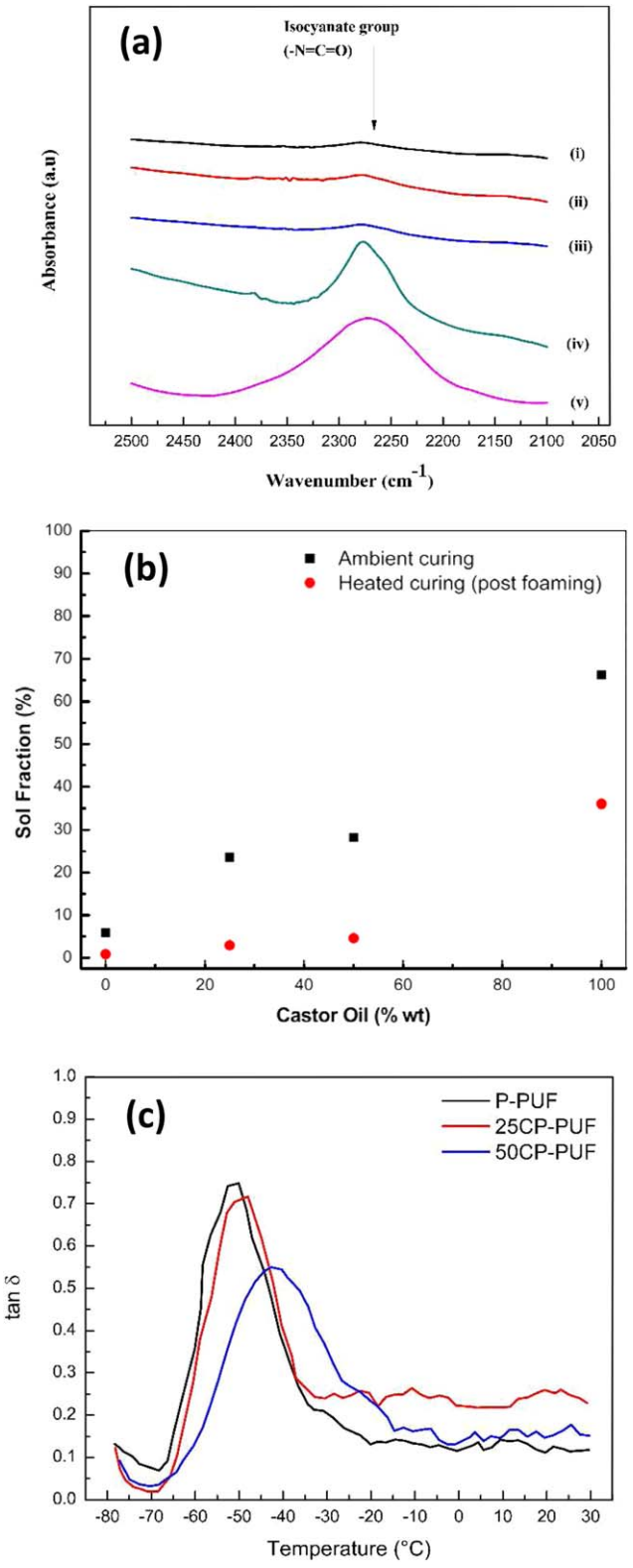

Figure 6. (a) Residual isocyanate in polymeric phase of foams: ((i) P-PUF; (ii) 25CP-PUF; (iii) 50CP-PUF; (iv) C-PUF; (v) C-PUF with NCO index at 100); (b) sol fraction in polymeric phase as a function of castor oil concentration in hydroxyl component: (c) dynamic mechanical analysis of foams. [Color figure can be viewed in the online issue, which is available at wileyonlinelibrary.com.]

spacing) in P-PUF is ~11.8 nm. The diffused, shoulder like peak seen in the case of *50*CP-PUF indicates that the fraction of scattering domains that are separated is very low. The increase in the size of domains in *50*CP-PUF is most probably due to the onset of coalescence of smaller discrete domains. Analyzing the observations from FTIR spectra together with AFM and SANS results, it is clear that the increase in castor oil concentration in the hydroxyl component results in the assembly of monodentate urea domains. The assembly becomes complete in the case of pure castor oil foams with the hard domains making a connected cluster in the continuous lamellar soft matrix.

Residual Oligomers, Sol Fraction, and Soft Domain Glass Transition Temperature. Figure 6(a) shows the FTIR spectra, in which the antisymmetric isocyanate stretching bands of foams are featured while in Figure 6(b) the sol fractions in the polymeric phase of the foam are shown. The areas of the peaks obtained after deconvolution of the spectra in Figure 6(a) are insignificant for P-PUF, and are small for *25*CP-PUF (0.8) and *50*CP-PUF (0.8), respectively. The estimated peak area for C-PUF is very high at 4.2. Foams made from pure polyether polyol have <6% of extractable content [Figure 6(b)], indicating very high network connectivity in the polymeric phase. The sol fraction in the polymeric phase of C-PUF is very high at around 66%, while on heated curing (post foaming) it reduces to around 36% [Figure 6(b)]. This futher reduction in sol fraction is due to reaction among residual oligomers, thereby enhancing the crosslink network at a later stage.

Figure 6(c) shows the dynamic mechanical behavior of the foams under a temperature ramp. The pure polyether polyol derived foam shows a tan δ peak at $-53°C$ with a peak intensity of 0.83 (peak height), attributed to the T_g of the soft domain. For *50*CP-PUF, the tan δ peak height decreases by 30% and the peak position shifts by 13°C. It would be worth analyzing the trends in T_g along with sol fraction and residual oligomeric fraction. Pure polyether polyol has a low hydroxyl value and high molecular weight (35 and 4700, respectively), whereas castor oil has high hydroxyl value (~163) and lower molecular weight (930). As a result, the chain length between two adjacent hydroxyl groups in castor oil is much lesser than that of polyether polyol. This should have facilitated the development of an extended network in the soft urethane phase derived from castor oil. The increase observed in T_g of partially substituted foams is due to this. The fact that these foams show a single T_g with much broader peak indicates considerable phase mixing between the soft domains generated from polyether polyol and castor oil. Going by the aforementioned argument, the use of pure castor oil should have facilitated the highest crosslink density and lowest concentration of loose macromolecules by means of an extended network in the polymeric phase. However, the sol fraction, in C-PUF shows an apparently contradicting trend and is the highest among all. It is also pertinent to note that due to the high sol fraction, DMA measurements could not be carried on C-PUF, as the foam collapsed under a dynamic ramp. Hence, the only plausible reason for highest sol fraction in C-PUF is due to the presence of unreacted oligomers and not due to non-network forming macromolecules. This is also clear from the high residual isocyanate content in C-PUF

Table I. Macroscopic Foam Stress Dissipation

Properties	P-PUF	*25*CP-PUF
Foam density (kg m^{-3})	48.4	48.3
Indentation force deflection (25%, kgf)	22.7	13.7
Indentation force deflection (40%, kgf)	34.6	21.0
Indentation force deflection (65%, kgf)	74.0	45.7

[Figure 6(a)]. This leads to the conclusion that the fractional conversion of castor oil during the reaction with isocyanate is less than unity. Thus, a significant volume of unreacted castor oil and isocyanate is present in C-PUF. The most probable reason for such less reactivity is due to the secondary nature of the hydroxyl component as well as the steric effects of the dangling chain that extends beyond the hydroxyl functional.[4]

Stoichiometric Matching of Hydroxyl to Isocyanate Groups. Finally, the effect of stoichiometry between hydroxyl and isocyanate functional groups would be worth exploring. It is very important to note that the foams described above were synthesized by keeping the weight ratio of isocyanate to hydroxyl component a constant at 65 : 100. This gives an isocyanate index of ~100 in the case of pure polyether polyol, indicating a 1 : 1 molar balance between —NCO and —OH groups. Because the hydroxyl value of castor oil is much higher, the increasing concentration of castor oil will decrease the isocyanate index for a constant weight fraction of oligomeric MDI. Based on this, the isocyanate indexes calculated for 25, 50, and 100% castor oil substituted foaming are ~91, 80, and 68, respectively. Thus, with increase in castor oil concentration, the stoichiometry NCO/OH becomes lesser than unity creating excess hydroxyl groups. As discussed above, due to the lesser reactivity of castor oil, there is always some residual amount of oligomers in foams synthesized from hydroxyl component having castor oil present in it. However, the deficiency of isocyanate moieties becomes acute in the case of foam synthesis with castor oil, where the isocyanate index is substantially low at 68. To see the effect of keeping the molar ratio between hydroxyl and isocyanate groups a constant, we have also synthesized foams from pure castor oil by keeping the isocyanate index at 100. This required increasing the weight of isocyanate used. Similar to foams made from pure castor oil with lesser isocyanate index, these foams were also unstable and collapsed. Because of the lack of foam structural integrity, mechanical testing and DMA could not be carried out on these foams. However, we measured the residual isocyanate and sol-fraction. The residual isocyanate is additionally shown in spectra no. v of Figure 6(a). Compared to the spectra no. iv of the same figure, which shows the residual isocyanate content of C-PUF made from an index of 68, the peak area shows substantial increase. This indicates that the effect of matching the molar ratio between the hydroxyl and isocyanate is an increase in residual isocyanate content. This increase in unconsumed isocyanate is obviously due to the less reactivity of hydroxyl groups of castor oil with —NCO groups. The sol fraction in C-PUF synthesized with an isocyanate index of 100 is found to be 14.9. This value is much lesser than for C-PUF synthesized from an isocyanate index of 68. This shows that as more isocyanate moieties are available for reacting with hydroxyl group, more castor oil gets consumed. However, the fact that the resultant foams were collapsed shows that sufficient conversion is still not achieved during the foaming period. This creates a lack of gel strength which adversely affects the foam stability. The additional conversion as shown by the decrease in sol-fraction most likely occurs in the post foaming period.

Macroscopic Stress Dissipation

The rate of network formation and phase separation in polyurethanes has significant bearing on the foam macroscopic properties.[41] The load bearing capacity of foam is a complex function of foam cellular and polymer phase morphologies. The bulk properties of solid foams are listed in Table I. Foams tested were molded to a constant overall density for comparison. Confined foaming with constant density ensures the molded foam cell morphology to be fairly uniform so that the bulk properties could be compared to the changes in polymer phase morphology. Beyond 25% of castor oil, the foams started showing internal defects so that the cellular morphology is no longer uniform and hence comparison of properties as a function of polymer phase morphology becomes difficult. The indentation force deflection at all levels of deflection for *25*CP-PUF shows an approximate decrease of 39% compared to C-PUF. Lower load bearing capacity indicates that the viscous dissipation in the foam is higher than the elastic recovery under an applied stress. The increase in sol fraction in *25*CPPUF can dissipate the applied stress. Moreover, the hard domains in a polyurethane matrix are considered to function similar to that of fillers that are connected with the lamellar matrix by entanglements.[42] It has been shown that when spheroid fillers are used to reinforce a polymer, it is the degree of interaction between the filler and the polymer matrix that contributes to the mechanical properties.[43] Hydrogen bonding between the urea hard domains and the polyether soft segments in C-PUF provide for such favorable interactions. In the case of castor oil, the aggregation of the hard domains reduces the available interfacial area of interaction between the two domains.

CONCLUSIONS

By conducting a gradual replacement of the conventional hydroxyl oligomer by castor oil, the microstructure and stability of polyurethane foams synthesized partially and completely from castor oil are investigated. The reductions in initial viscosity of reacting oligomers followed by a drastic drop in the transient development of liquid matrix modulus reduce the foam stability, especially at high castor oil concentrations. Foams became relatively more stable when the foaming reaction was deferred to a stage, where sufficient modulus was developed. Foams synthesized completely from castor oil were unstable in all the cases. The entire fraction of free urea in conventional foams is converted to hydrogen bonded monodentate urea in pure castor oil foams. These urea domains undergo self assembly in pure castor oil based foams, significantly altering the entire segmented morphology. Partially substituted foams show moderate increase in glass transition temperature with possible phase mixing between the castor oil and polyether polyol generated urethane domains. Foams generated from pure castor oil

are highly unstable due to significant amount of unreacted oligomers. Pure castor oil foams made by matching the stoichiometry between isocyanate and hydroxyl group were also unstable and collapsed, indicating the inferior reactivity of castor oil with isocyanate. The changes in foam and polymeric phase morphologies reduce the load bearing property of partially substitute foams.

ACKNOWLEDGMENTS

Financial support from UGC-DAE Consortium for Scientific Research through grant number CRS-M-171 and the beam time provided at the neutron scattering facilities of Dhruva Reactor, Bhabha Atomic Research Centre, Mumbai are acknowledged. The authors are grateful to Huntsman Polyurethanes for materials and load bearing property measurements. The authors thank Prof. Rabibrata Mukherjee and Sayantani Saha for AFM imaging and S. Praveen for DMA. Parts of this work were carried out at the central research facility of the Indian Institute of Technology, Kharagpur.

REFERENCES

1. Randall, D.; Lee, S. The Polyurethanes Book, 2nd ed.; Wiley-Interscience: New York, **2002**; p 2.
2. Calcagnile, P.; Fragouli, D.; Bayer, I. S.; Anyfantis, G. C.; Martiradonna, L.; Cozzoli, P. D.; Cingolani, R.; Athanassiou, A. *ACS Nano.* **2012**, *6*, 5413.
3. Petrovic, Z. S. *Polym. Rev.* **2008**, *48*, 109.
4. Pfister, D. P.; Xia, Y.; Larock, R. C. *Chem. Sus. Chem.* **2011**, *4*, 703.
5. Babb, D. A. *Adv. Polym. Sci.* **2012**, *245*, 315.
6. Javni, I.; Petrovic, Z. S.; Guo, A.; Fuller, R. J. *J. Appl. Polym. Sci.* **2000**, *77*, 1723.
7. Petrovic, Z. S.; Cevallos, M. J.; Javni, I.; Schaefer, D. W.; Justice, R. J. *J. Polym. Sci. B Polym. Phys.* **2005**, *43*, 3178.
8. Kong, X.; Yue, J.; Narine, S. S. *Biomacromolecules* **2007**, *8*, 3584.
9. Zlatanic, A.; Lava, C.; Zhang, W.; Petrovic, Z. S. *J. Polym. Sci. B Polym. Phys.* **2004**, *42*, 809.
10. Bahr, M.; Mulhaupt, R. *Green Chem.* **2012**, *14*, 483.
11. Guruswamy-Thangavelu, S. A.; Emond, S. J.; Kulsreshta, A.; Hillmyer, M. A.; Macosko, C. W.; Tolman, W. B.; Hoye, T. R. *Polym. Chem.* **2012**, *3*, 2941.
12. Pechar, T. W.; Sohn, S.; Wilkes, G. L.; Ghosh, S.; Frazier, C. E.; Fornof, A.; Long, T. E. *J. Appl. Polym. Sci.* **2006**, *101*, 1432.
13. Xia, Y.; Zhang, Z.; Kessler, M. R.; Brehm-Stecher, B.; Larock, R. C. *Chem. Sus. Chem.* **2007**, *5*, 2221.
14. Tan, S.; Abraham, T.; Ference, D.; Macosko, C. W. *Polymer* **2011**, *52*, 2840.
15. Zhang, C.; Xia, Y.; Chen, R.; Huh, S.; Johnston, P. A.; Kessler M. R. *Green Chem.* **2013**, *15*, 1477.
16. Zhang, L.; Jeon, H. K.; Malsam, J.; Herrington, R.; Macosko, C. W. *Polymer* **2007**, *48*, 6656.
17. Yeganeh, H.; Mehdizhadeh, M. R. *Eur. Polym. J.* **2004**, *40*, 1233.
18. Petrovic, Z. S.; Hong, D.; Javni, I.; Erina, N.; Zhang, F.; Llavski, J. *Polymer.* **2013**, *54*, 372.
19. Lyon, C. K.; Garret, V. H.; Goldblatt, L. A. *J. Am. Oil. Chem. Soc.* **1962**, *39*, 69.
20. Lyon, C. K.; Garret, V. H.; Goldblatt, L. A. *J. Am. Oil. Chem. Soc.* **1962**, *41*, 23.
21. Baser, S. A.; Khakhar, D. V. *Cell. Polym.* **1993**, *12*, 390.
22. Wang, H. J.; Rong, M. Z.; Zhang, M. Q.; Hu, J.; Chen, H. W.; Czigany, T. *Biomacromolecules* **2008**, *9*, 615.
23. Palanisamy, A.; Rao, B. S.; Mehazabeen, S. J. *Polym. Environ.* **2011**, *19*, 698.
24. Available at: http://www.basf.com/group/corporate/en_GB/function/conversions:/publish/content/sustainability/eco-efficiency-analysis/images/Lupranol_BALANCE_EEA.pdf (retrieved on 26 September 2013).
25. Vaughan, B. R.; Wilkes, G. L.; Dounis, D. V.; Mclaughlin, C. *J. Appl. Polym. Sci.* **2011**, *119*, 2684.
26. Ogunleye, O. O.; Oyawale, F. A.; Suru, E. *Global J. Biotech. Biochem.* **2007**, *2*, 28.
27. Zheng, C.; Han, X.; Lee, L. J.; Koelling, K. W.; Tomasko, D. L. *Adv. Mater.* **2003**, *15*, 1743.
28. Zhang, L. Structure–Property Relationship of Polyurethane Flexible Foam Made from Natural Oil Polyols, Ph.D. Thesis; University of Minnesota: Minneapolis, MN, USA, **2008**.
29. Macosko C. W. RIM: Fundamentals of Reaction Injection Molding; Hanser Publishers: New York, **1989**; p 1.
30. Harikrishnan, G.; Khakhar, D. V. *AIChE J.* **2010**, *56*, 522.
31. Zhang, X. D.; Macosko, C. W.; Davis, H. T.; Nikolov, A. D.; Wasan, D. T. *J. Colloid Interface Sci.* **1999**, *215*, 270.
32. Velankar, S.; Kooper, S. L. *Macromolecules* **1998**, *31*, 9181.
33. O'Stickey, M. J.; Lawrey, B. D.; Wilkes, G. L. *Polymer* **2002**, *43*, 7399.
34. Kaushiva, B. D.; Wilkes, G. L. *Polymer* **2000**, *41*, 6981.
35. Li, W.; Ryan, A. J.; Meier, I. K. *Macromolecules* **2002**, *35*, 6306.
36. Elwell, M. J.; Ryan, A. J.; Grünbauer, H. J. M.; Van Leiehout, H. C. *Polymer* **1996**, *37*, 1353.
37. Luo, N.; Wang, D. N.; Ying, S. K. *Macromolecules* **1997**, *30*, 4405.
38. Yilgor, E.; Yilger, I.; Yurtsever, E. *Polymer* **2002**, *43*, 6551.
39. Dounis, D. V.; Wilkes, G. L. *Polymer* **1997**, *38*, 2819.
40. Kurt, P.; Gamble, L. J.; Wynne, K. J. *Langmuir* **2008**, *24*, 5816.
41. Wilkes, G. L.; Emerson, J. A. *J. Appl. Phys.* **1976**, *47*, 4261.
42. Mang, J. T.; Hjelm, R. P.; Orler, E. B.; Wrobleski, D. A. *Macromolecules* **2008**, *41*, 4358.
43. Sternstein, S. S.; Zhu, A. J. *Macromolecules* **2002**, *35*, 7262.